Available online at www.sciencedirect.com

ScienceDirect

Procedia Structural Integrity 12 (2018) 353–369

Structural Integrity Procedia

www.elsevier.com/locate/procedia

AIAS 2018 International Conference on Stress Analysis

Comparison of numerical models for Acoustic Emission propagation

A. Chiappa[a,*], F. Giorgetti[a], A. Marzani[b], M. Messina[b], G. Augugliaro[c], C. Mennuti[c], M. E. Biancolini[a]

[a]*Department of Enterprise Engineering "Mario Lucertini", University of Rome "Tor Vergata", Via del Politecnico 1, 00133, Roma*
[b]*Department of Civil, Chemical, Environmental and Materials Engineering, DICAM, University of Bologna, Viale del Risorgimento 2, 40136, Bologna*
[c]*Istituto Nazionale per l'Assicurazione contro gli Infortuni sul Lavoro, INAIL, Via di Fontana Candida 1, 00040, Monte Porzio Catone, Roma*

Abstract

Acoustic Emissions (AE) are at the basis of extremely accurate and reliable monitoring systems. Within the SmartBench project, data regarding structural health of components are gathered in a database in order to make safety integrated, operative and smart. An accurate modelling of wave propagation is a necessary requirement for a proper design of sensor networks as well as for data interpretation. Numerical simulations of the transient behavior of structural systems are well-established in this field but, on the minus side, they are very expensive in terms of computational time and resources. This paper reports different instances of AE propagation through metallic media. Bulk waves and guided waves are both investigated by means of 2D and 3D models and resorting to different software. Obtained results are cross-checked and computational times are compared as well. As a last point, High Performance Computing is applied to the case of waves simulation in order to get a significant reduction of the required computational time.

Keywords: Ultrasonic waves; numerical simulation; Finite Element Method; COMSOl; ANSYS; FEMAP; NASTRAN.

*Corresponding author. Tel.: +39 06 72597136
E-mail address: andrea.chiappa@uniroma2.it

10.1016/j.prostr.2018.11.081

1. Introduction

Ultrasonic guided waves (UGW) turned out to be an effective way for nondestructive evaluation (NDE) and structural health monitoring (SHM) of the structures acting as waveguides. They bring undeniable advantages with respect to bulk waves, such as a wider inspection capability and a major versatility. Their action is particularly appreciated for the scanning of beam-like or plate-like structures such as pipes, railroad tracks or laminates, as in the works by Lowe et al. (1998) and Leckey et al. (2018). Whether bulk waves or guided waves propagate in a medium depends upon the ratio of the wavelength on the domain dimensions, as described in Rose (2014). When wavelength is greater than the structural thickness, boundaries play a fundamental role and guided waves are generated. Otherwise waves behave as in an infinite medium, leading to bulk waves. Structural assessment by means of UGW can take advantage of two different phenomena, both involving waves propagation. The first is due to the reflection and modification of an induced signal when it encounters a flaw. The second relies on the spontaneous emission of acoustic vibrations at the onset or during the evolution of a crack. On the minus side, UGW present a dispersive behavior which needs to be fully understood in order to exploit their advantages. The effect of dispersion is due to the dependency of the phase velocity on frequency and the existence of different modes. Each mode is characterized by its own dispersion curve and a single excitation frequency can involve multiple modes. A former work by Gavrić (1994) deals with a method for the computation of dispersion curves of thin-walled structures (such as cylinders or beams of I-shaped cross sections) based on finite elements (FE). The FE models are built with proper shell elements. In a subsequent paper by the same Gavrić (1995), the same approach is applied to solid waveguides. It requires a FE discretization of the cross-section of the waveguide alone while an analytical form is assumed for the displacement field along the propagation direction (semi-analytical finite element method). The method is there employed for the case of a free rail. In a paper by Wilcox et al. (2002), a smart way is proposed to apply the technique presented by Gavrić: dispersion curves for an arbitrary cross-section can be worked out resorting to a FE package allowing cyclic symmetry. The so-called semi-analytical finite element (SAFE) method demonstrated its effectiveness to catch the transmission features of dispersive solid media. A recent upgrade of this approach is presented by Bartoli et al. (2006). Accordingly to previous works, the SAFE method assumes the periodicity of the wave propagation along the guide. Damping effects are kept into account with a complex form for the stiffness matrix. Instances of the proposed method are presented, including viscoelastic anisotropic media and laminates. In a work by Marzani et al. (2008) the SAFE method is extended to axisymmetric waveguides with damping. Cylindrical coordinates are introduced in order to adopt a mono-dimensional approach for discretization. The semi-analytical method is a useful tool to characterize the propagative and evanescent modes in waveguides but it does not give any information on the waveforms or on the displacement scenario at a given moment of time. If such knowledge is sought, a transient FE analysis is still the unique choice, as presented by Bartoli et al. (2005). This last paper reports an interesting study on the use of guided waves for defect detection in railroads tracks. Numerical results obtained by ABAQUS EXPLICIT are found in good agreement with the experimental ones. As a preliminary step, a theoretical test-case is employed to validate the existing guidelines for the spatial and temporal discretization. A FE technique to model guided waves propagation is described by Moser et al. (1999). The analytical solution for the case of a flat plate is used as a benchmark to prove the soundness of the numerical approach. A thick ring is studied as a waveguide and the results are validated against theoretical considerations. Further checks come from the comparison with the mode superimposition method and experimental waveforms. The work presented by Leckley (2018) reports a cross-check of results obtained by different software for guided-wave propagation in a laminate composite. A delamination flaw is considered and experimental data are compared to numerical simulations: ABAQUS, ANSYS, COMSOL and an in-house code are employed for the case. In general a good matching is observed, but important differences arise in terms of computational running time, with COMSOL outperforming the other tested software.

The Smartbench project (www.smartbench-project.it) involves different Italian partners: the University of Rome "Tor Vergata", the University "Campus Bio-Medico" of Rome, the University of Bologna UNIBO, the University of Salento and the University of Messina as academic foundations. INAIL, the Italian public body of job insurance, rounds out the group. The overall goal of the project is to introduce a technological change in job security in an integrated fashion. Different tools must be synchronized to this end: networks of Acoustic Emissions (AE) sensors for a continuous monitoring of the structural health of components, smart tags to manage work equipment and facilities, virtual simulation of ageing of structures, and internet of things (IOT) to assess the personnel health state

and the proper use of the protective equipment. The present work focuses on the AE topic: it reports a comparison of results of FE analyses simulating ultrasonic waves propagation. Three commercial codes: COMSOL, ANSYS APDL and FEMAP with NX NASTRAN are compared for the purpose. Several instances are considered: bulk and guided waves propagation in 2D models and the dispersive behavior of a 3D plate.

Nomenclature

b_e	edge of the element of the numerical grid
c_g	group velocity of the wave packet at a given frequency
c_{ph}	phase velocity of the wave at a given frequency
c_L	velocity of longitudinal bulk waves
c_T	velocity of shear bulk waves
d	generic distance
f	frequency
h	half thickness of the plate of the Lamb problem
k	wavenumber
L	numerical domain edge
p	first parameter of the Lamb problem
q	second parameter of the Lamb problem
t	generic time instant
Δt	time step used for numerical integration
λ	wavelength
ω	circular frequency

2. Numerical tests

The present section reports the FE settings and the results obtained for scenarios of increasing complexity of ultrasonic wave propagation. The numerical simulation tools employed in this study are three widely used commercial FE codes: COMSOL, ANSYS APDL and FEMAP with NX NASTRAN. Theoretical considerations are reported in each dedicated sub-section, introducing propagation velocities to assess numerical results. In this work different dimensionalities of the propagation domains are investigated: a 2D model under the assumption of plane strain is considered for both bulk and guided waves, a fully 3D scenario is employed for guided waves only. All the considered codes rely on an implicit integration algorithm to solve the transient problem: Generalized-α for COMSOL, the Newmark algorithm for APDL and an approach similar to the Newmark-Beta method for NX NASTRAN. Unless otherwise specified, the reported running times are for a Dell Precision T5810 with a 3.50 GHz processor, 48.0 GB of RAM and 6 working cores.

2.1. Bulk waves propagation in a 2D domain

The first comparison involves the propagation of bulk waves. For this purpose, a proper domain is considered. A thick block of steel is modelled in 2D thanks to the assumption of plane strain. The material properties are the following:

- Young's modulus E = 209 GPa
- Poisson's ratio = 0.3
- Density ρ = 7800 Kg/m^3

The associated bulk propagation presents longitudinal wave velocity c_L = 6005.8 m/s and shear wave velocity c_T = 3210.3 m/s. Damping effects are neglected, a unitary thickness is chosen for the model. The whole domain is assumed to be a rectangle with stress-free boundaries, stimulated by a time-dependent force acting orthogonal at the

midpoint of its upper edge. Given the symmetry, only one half of the rectangle is modelled. The simulation domain is thus a square with a force acting at its upper-left vertex and a symmetry constraint along its left edge. The symmetry constraint just prescribes a zero motion normal to the considered edge. The force employed to start wave propagation has a prescribed evolution in time, which is reported in Fig. 1. It is a sine function with frequency f_0 = 50kHz, windowed by a Hann function with non-zero interval from $t = 0$ to $t_{Hann} = 8 \cdot 10^{-5}$ s. The simulations are run from $t = 0$ to $t_{end} = 4 \cdot 10^{-4}$ s. Given the bulk wave velocities and the frequency of the forcing function, the wavelengths of longitudinal and shear waves are $\lambda_L = c_L / f_0 = 0.12$ m and $\lambda_T = c_T / f_0 = 0.064$ m respectively. The edge L of the square domain is chosen to be 10 times λ_L, $L = 10 \cdot \lambda_L = 1.2$ m.

A critical aspect when dealing with numerical models is discretization, both temporal and spatial. In the case of ultrasonic waves simulation, this is even more true. In a paper by Bartoli et al. (2005), it is stated that the size of the finite element b_e should be tuned on the smallest wavelength to be analyzed λ_{min}. A spatial resolution from a minimum of 10 to a maximum of 20 nodes per wavelength is recommended.

$$\frac{\lambda_{\min}}{10} \le b_e \le \frac{\lambda_{\min}}{20} \tag{1}$$

As regards the time step Δt, the most stringent condition between (2) and (3) should be employed, being f_{max} the maximum frequency of the dynamic problem.

$$\Delta t = \frac{b_{e,\min}}{c_L} \tag{2}$$

$$\Delta t = \frac{1}{20 \cdot f_{\max}} \tag{3}$$

In a work by Moser et al. (1999) the upper limit of 20 subdivisions in (1) is said to be too strict and it is shown that spatial discretization is less critical than time stepping. In Leckley (2018) a discretization of just 8 nodes per wavelength is found satisfactory, while it is introduced a Courant number of 0.58 multiplying the right term in (2). It seems reasonable that each software requires a proper discretization in order to work at best, some trials being necessary to find this tuning. For the present case of bulk propagation, several settings were tried with three different commercial FE codes: COMSOL, ANSYS APDL and FEMAP with NX NASTRAN. An easy and practical way to assess the numerical results is to check propagation velocities. Waves are generated at a given point in the material, a probe placed at a certain distance receives a signal after a time which is determined by the distance to velocity ratio. Requested output of each numerical analysis is the displacement over time of the center point of the square domain, at a distance $d = 0.85$ m from the trigger site. As stated before, the excitation force acts in the interval of the Hann window, being zero outside. The arrival of longitudinal waves travelling the straight path to the probe is restricted to the interval $[t_{1L} \quad t_{2L}]$:

$$t_{1L} = \frac{d}{c_L} = 1.414 \cdot 10^{-4} \text{ s}$$

$$t_{2L} = t_{Hann} + \frac{d}{c_L} = 2.214 \cdot 10^{-4} \text{ s} \tag{4}$$

Analogously, for shear waves we use the bulk shear velocity to compute the interval $[t_{1T} \quad t_{2T}]$:

$$t_{1T} = \frac{d}{c_T} = 2.646 \cdot 10^{-4} \text{ s}$$

$$t_{2T} = t_{Hann} + \frac{d}{c_T} = 3.446 \cdot 10^{-4} \text{ s} \tag{5}$$

These bounds allow to have a check of the soundness of numerical results. Since different recommendations can be found in literature as regards discretization, we started with the stricter conditions given by (1), taking 20 nodes per wavelength, and (2), with a Courant number of 0.25 multiplying the right hand side. These guidelines yield to b_e = 0.0032 m and $\Delta t = 1.33 \cdot 10^{-7}$ s. The domain was discretized by 4-node bilinear square elements. Fig. 2 reports the components of displacement for the probe over time, obtained by COMSOL, APDL and FEMAP. The red and green lines represent the time bounds for the arrival of longitudinal and tangential waves given by (4) and (5). Oscillations crossing the second green line are due to waves bouncing back from the boundaries. All the commercial codes gave similar results, fulfilling the check of velocities.

The coarser spatial discretization given by 10 nodes per wavelength was also tried. The integration time step came consequently from (2), the Courant number was still 0.25, yielding to b_e = 0.0064 m and $\Delta t = 2.66 \cdot 10^{-7}$ s. In this second case, COMSOL showed a numerical anomaly: the arrival of tangential waves was anticipated in time, as reported in Fig. 3. APDL and FEMAP still respected the check of velocities. The separate study of spatial and temporal discretization showed that they offset each other. A coarser mesh anticipates the arrival of the waves, a larger time step introduces a delay. This suggests that a proportionality should be kept between the spatial and temporal paces. Former tests are repeated, the Courant number is set unitary so that Δt is exactly the one reported in (2), the discretization paces are b_e = 0.0064 m and $\Delta t = 1 \cdot 10^{-6}$ s. In Fig. 4, the probe displacements obtained in this second case. As regards COMSOL, anticipation of tangential waves is still present nonetheless its effect is less evident than before. Oscillations obtained with APDL are centered in the expected intervals, a delay can be noticed for the longitudinal waves reproduced by FEMAP. A larger time step was not tried because it would not have respected the Nyquist criterion in (3) with the given tolerance. Tables Table 1 and Table 2 reports the analyses parameters and running times for both the presented cases of discretization.

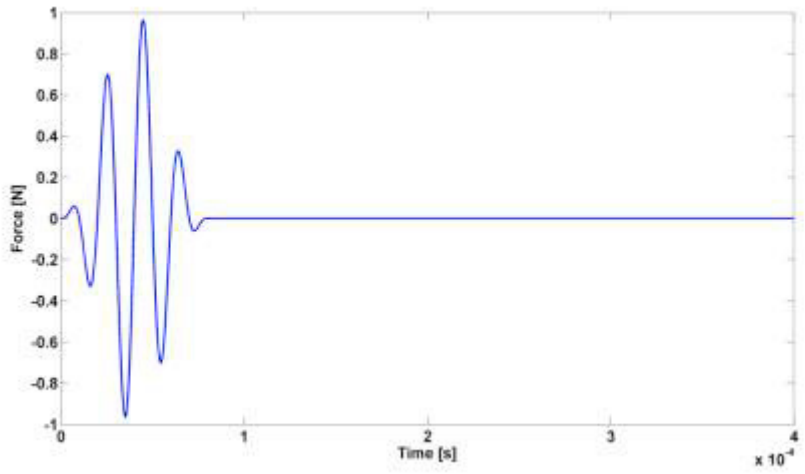

Fig. 1. Evolution over time of the forcing function.

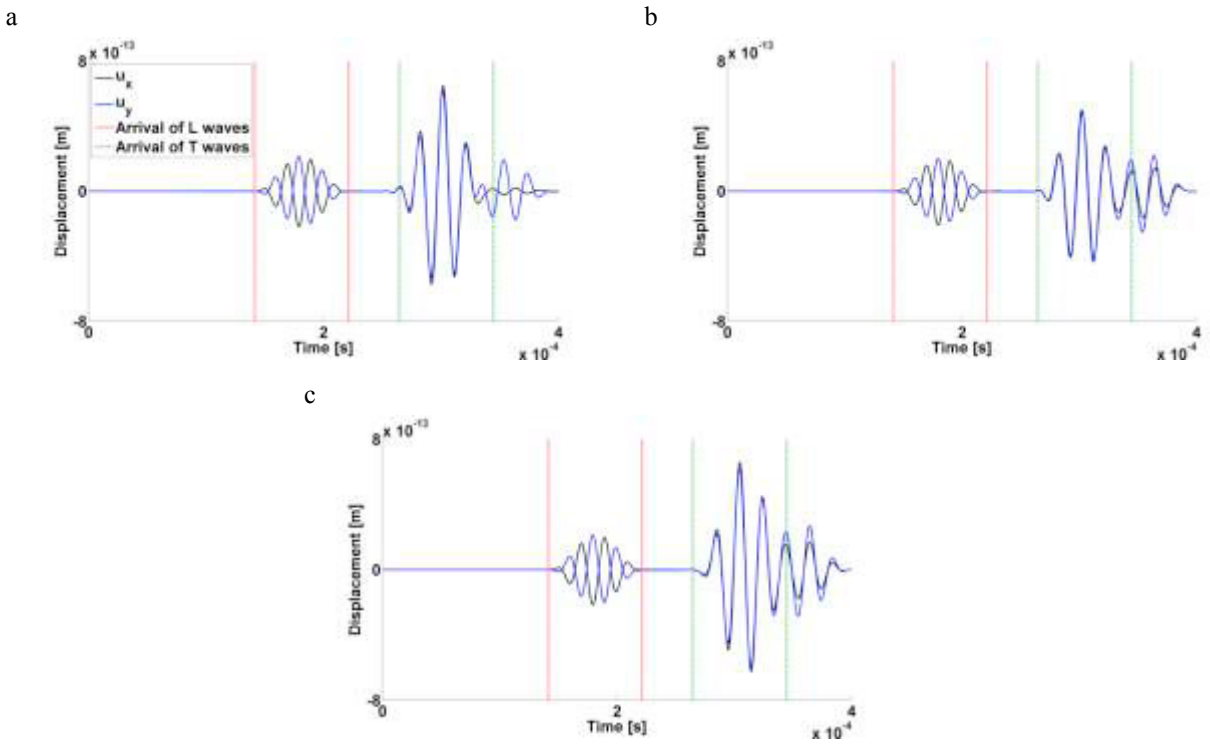

Fig. 2. Results of the first set of simulations for the 2D bulk case: (a) COMSOL; (b) APDL; (c) FEMAP.

Table 1. First set of simulations for the 2D bulk case: analysis parameters and running times.

Employed code	Element edge [m] b_e	Time step [s] Δt	Number of elements	Running time [s]
COMSOL	$3.2 \cdot 10^{-3}$	$1.33 \cdot 10^{-7}$	140625	1339
APDL	$3.2 \cdot 10^{-3}$	$1.33 \cdot 10^{-7}$	141376	2600
FEMAP	$3.2 \cdot 10^{-3}$	$1.33 \cdot 10^{-7}$	139876	3279

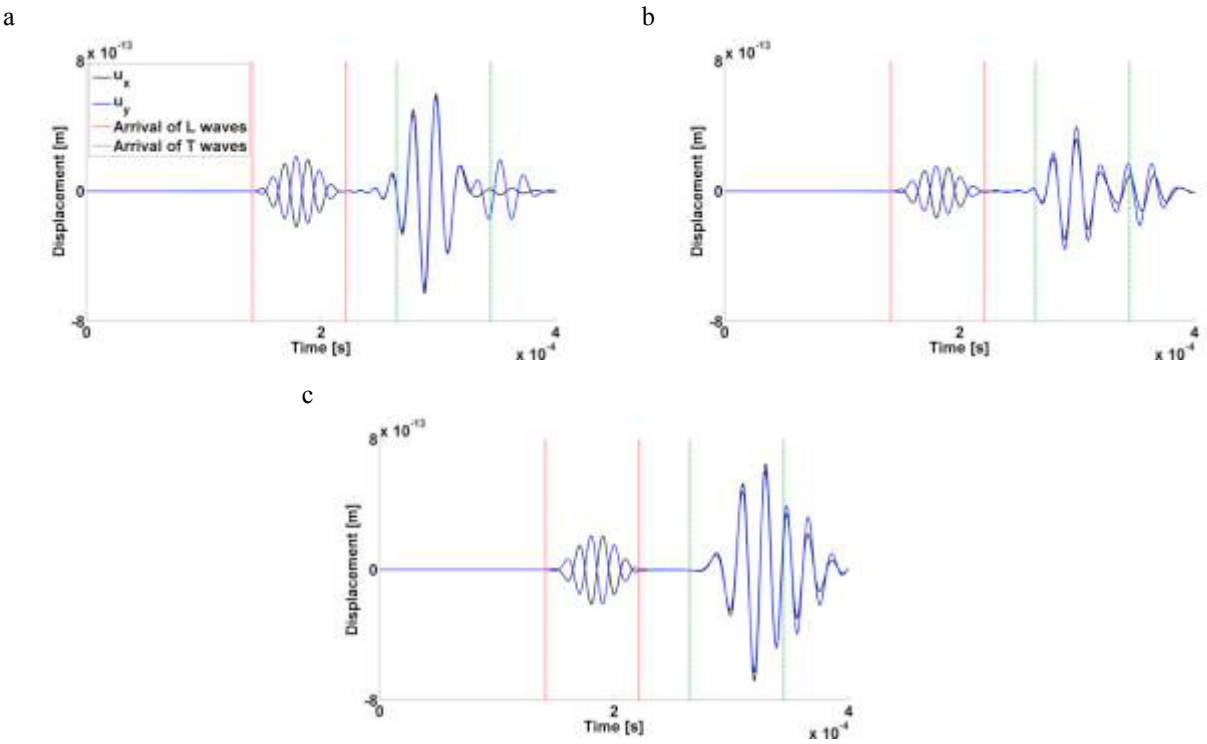

Fig. 3. Results of the second set of simulations for the 2D bulk case: (a) COMSOL; (b) APDL; (c) FEMAP.

Table 2. Third set of simulations for the 2D bulk case: analysis parameters and running times.

Employed code	Element edge [m] b_e	Time step [s] Δt	Number of elements	Running time [s]
COMSOL	$6.4 \cdot 10^{-3}$	$1 \cdot 10^{-6}$	35344	44
APDL	$6.4 \cdot 10^{-3}$	$1 \cdot 10^{-6}$	35344	91
FEMAP	$6.4 \cdot 10^{-3}$	$1 \cdot 10^{-6}$	35344	375

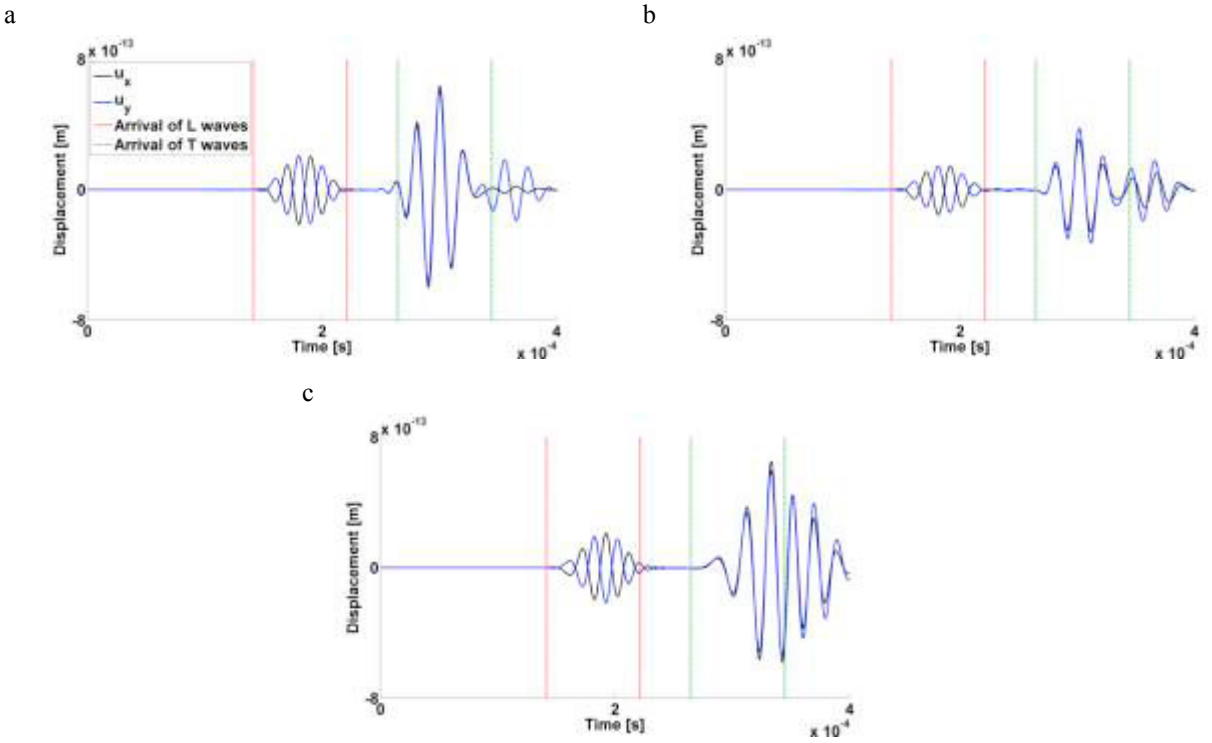

Fig. 4. Results of the third set of simulations for the 2D bulk case: (a) COMSOL; (b) APDL; (c) FEMAP.

2.2. Guided waves propagation in a 2D domain

As reported in the introduction, the physics of UGW is definitely more complex than that of bulk waves. The velocities of UGW depend upon the geometry of the waveguide while several modes can be involved. Transmission of waves travelling in a thin plate of isotropic material, with stress-free boundaries under the assumption of plane strain is the classical problem of Lamb waves propagation. The well-known Rayleigh-Lamb solutions of Lamb waves can be found in Rose (2014):

$$\frac{\tan(qh)}{\tan(ph)} = -\frac{4k^2pq}{\left(q^2-k^2\right)^2} \quad \text{for the symmetric modes} \tag{6}$$

$$\frac{\tan(qh)}{\tan(ph)} = -\frac{\left(q^2-k^2\right)^2}{4k^2pq} \quad \text{for the anti-symmetric modes}$$

where k is the wavenumber, $2h$ is the plate thickness.

The parameters p and q derive from the circular frequency ω, the wavenumber k and the aforementioned bulk velocities:

$$p^2 = \left(\frac{\omega}{c_L}\right)^2 - k^2$$

and (7)

$$q^2 = \left(\frac{\omega}{c_T}\right)^2 - k^2$$

If waves characteristics are sought for a generic cross-section of the waveguide, no analytical solution exists, justifying the recourse to semi-analytical or numerical methods. In this work the tool Guiguw (available at www.guiguw.com) was employed for the purpose. It is a software able to supply the dispersion curves for both the Lamb waves problem and for a generic cross-section waveguide. The SAFE method, described by Bartoli et al. (2006), constitutes its working core.

The case under consideration perfectly matches the Lamb problem requirements. It is the first example considered in a work by Bartoli et al. (2005). It is a 2D thin plate, 3 m long and 2 cm thick, supposed infinite along the wideness with traction-free upper and lower surfaces. An ultrasonic excitation occurs at one edge of the plate in the form of an impulsive displacement along the length, for a duration of 20 μs, as represented in Fig. 5a. The amplitude spectrum of the impulse is reported in Fig. 5b. It shows that the upper bound of the frequency range of interest can be placed at 100 kHz. Dispersion curves obtained by Guiguw (Fig. 6) reveal that in the considered frequency interval, only zero-order symmetric mode S_0 and anti-symmetric mode A_0 are present. The starting push excites the plate in a symmetrical manner with respect to its longitudinal mid-plane, thus only the symmetric mode propagation S_0 is activated (black curve). The material is steel, the same previously considered. As a first attempt, the discretization given in referenced paper was tried, the package used in the cited work was ABAQUS EXPLICIT. Under the assumption of plane strain, 4-nodes square elements with edge b_e = 10 mm were considered. The integration time step was set to $\Delta t = 2 \cdot 10^{-7}$ s. The observation of Lamb dispersion curves revealed that, in the frequency interval of interest, the phase velocity of symmetric waves ranges from $c_{ph,1}$ = 5459 m/s for a near-zero frequency to $c_{ph,2}$ = 4942 m/s for a frequency of 100 kHz. Dealing with guided waves, it is correct to consider group velocities. The group velocity is the propagation velocity of a group of waves of similar frequency. It is associated with the motion of the waves packets or envelopes. In the considered zone of the graph, the group velocity decreases from $c_{g,1}$ = 5394 m/s to $c_{g,2}$ = 3489 m/s, the wavelength shifts from λ_1 = 545.9 m at 0 kHz, to λ_2 = 0.049 m at 100 kHz. The variable monitored was the longitudinal displacement of the node at the mid-span of the top surface, at a distance d = 1.5 m from the stimulated edge. The simulations were run from t = 0 to $t_{end} = 1.3 \cdot 10^{-3}$ s. The arrival window $[t_1 \quad t_2]$ is evaluated according to the considerations valid also for bulk waves, when the group velocities are considered:

$$t_1 = \frac{d}{c_{g,1}} = 2.781 \cdot 10^{-4} \text{ s}$$

(8)

$$t_2 = 20[\mu\text{s}] + \frac{d}{c_{g,2}} = 4.499 \cdot 10^{-4} \text{ s}$$

Fig. 7 reports the displacement over time for the selected node obtained by COMSOL, APDL and FEMAP. COMSOL and APDL slightly anticipated the arrival of symmetric waves with a negative peak of the displacement

just before the red line, showing a similar shape of the oscillations. The signal reported by FEMAP is better centered in the expected interval and its shape is much more similar to that shown in the referenced literature. The second oscillation which appears in the figures is due to the reflection from the right-end of the plate. The numerical tests were repeated with a different spatial and temporal resolutions. The guidelines found for the bulk case were applied also for the instance of guided waves. It was found that a proportionality should hold between the spatial and the time steps. The interval reported in (1) is well balanced by the time pace given in (2) with unitary Courant number. A discretization of 20 nodes per wavelength was adopted since:

i) its related time step satisfies the Nyquist criterion given in (3)
ii) the area to be meshed had a small extent

For the second set of numerical analyses the parameters $b_e = \lambda_2/20 = 0.0025$ m, $\Delta t = b_e/c_{g,1} = 4.6 \cdot 10^{-7}$ s were employed. Fig. 8 reports the monitored displacement obtained by COMSOL, APDL and FEMAP for the last introduced discretization. All the curves appear similar and the peaks are well centered in the expected interval. Tables Table 3 and Table 4 summarize the parameters of interest of the discussed analyses and the related running times.

a b

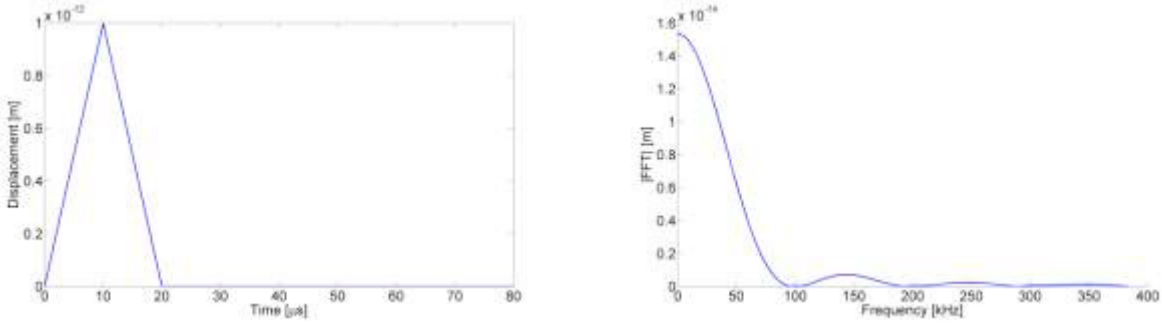

Fig. 5. (a) Displacement over time of the impulse; (b) frequency spectrum of the impulse.

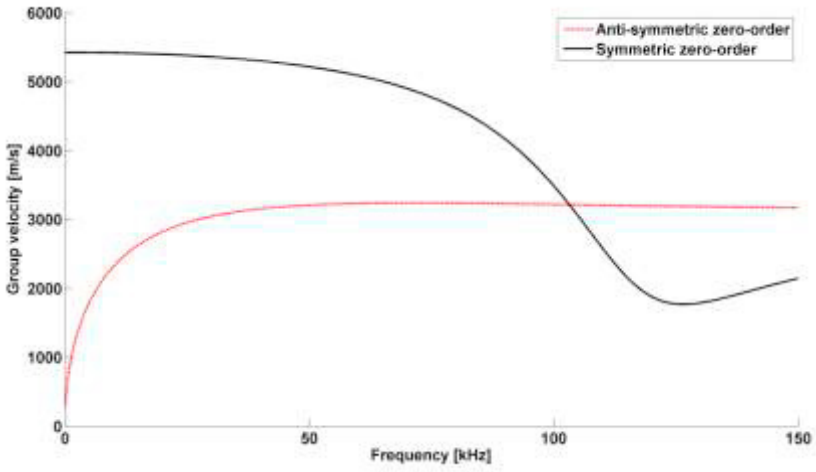

Fig. 6. Group velocity vs frequency for the 2D guided propagation problem.

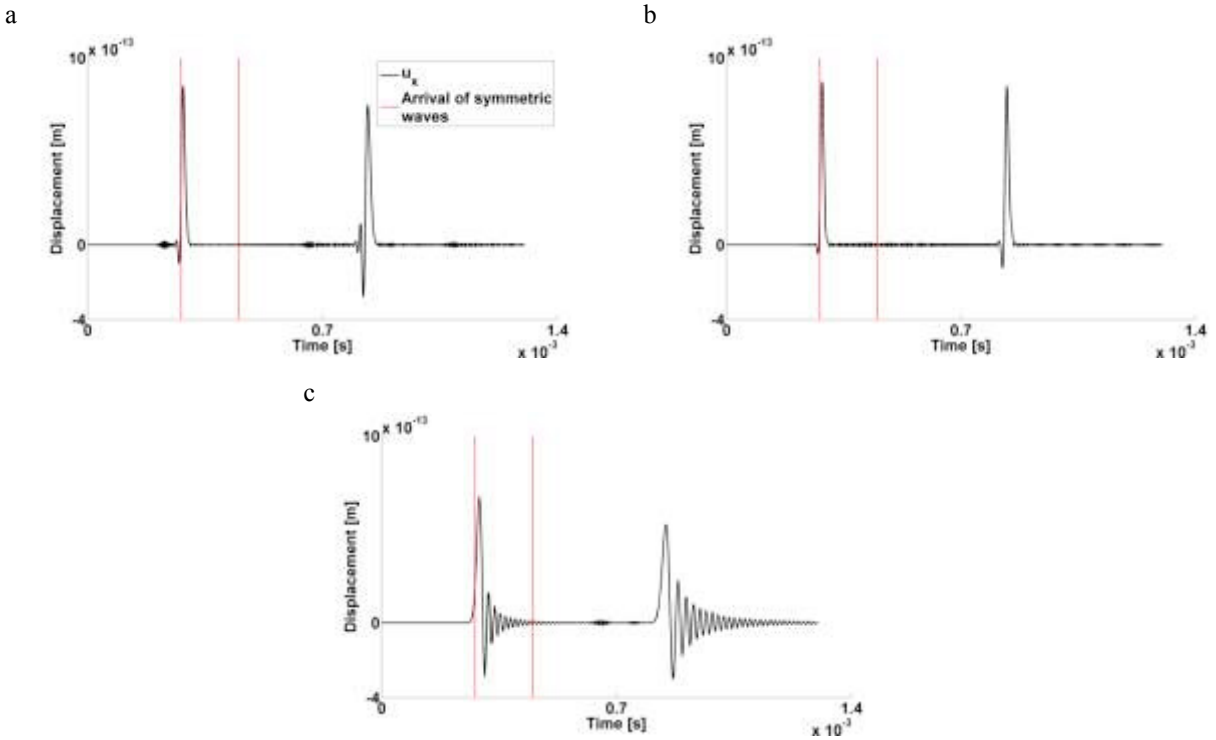

Fig. 7. Results of the first set of simulations for the 2D guided propagation case: (a) COMSOL; (b) APDL; (c) FEMAP.

Table 3. First set of simulations for the 2D guided propagation case: analysis parameters and running times.

Employed code	Element edge [m] b_e	Time step [s] Δt	Number of elements	Running time [s]
COMSOL	$10 \cdot 10^{-3}$	$2 \cdot 10^{-7}$	600	32
APDL	$10 \cdot 10^{-3}$	$2 \cdot 10^{-7}$	600	64
FEMAP	$10 \cdot 10^{-3}$	$2 \cdot 10^{-7}$	600	5

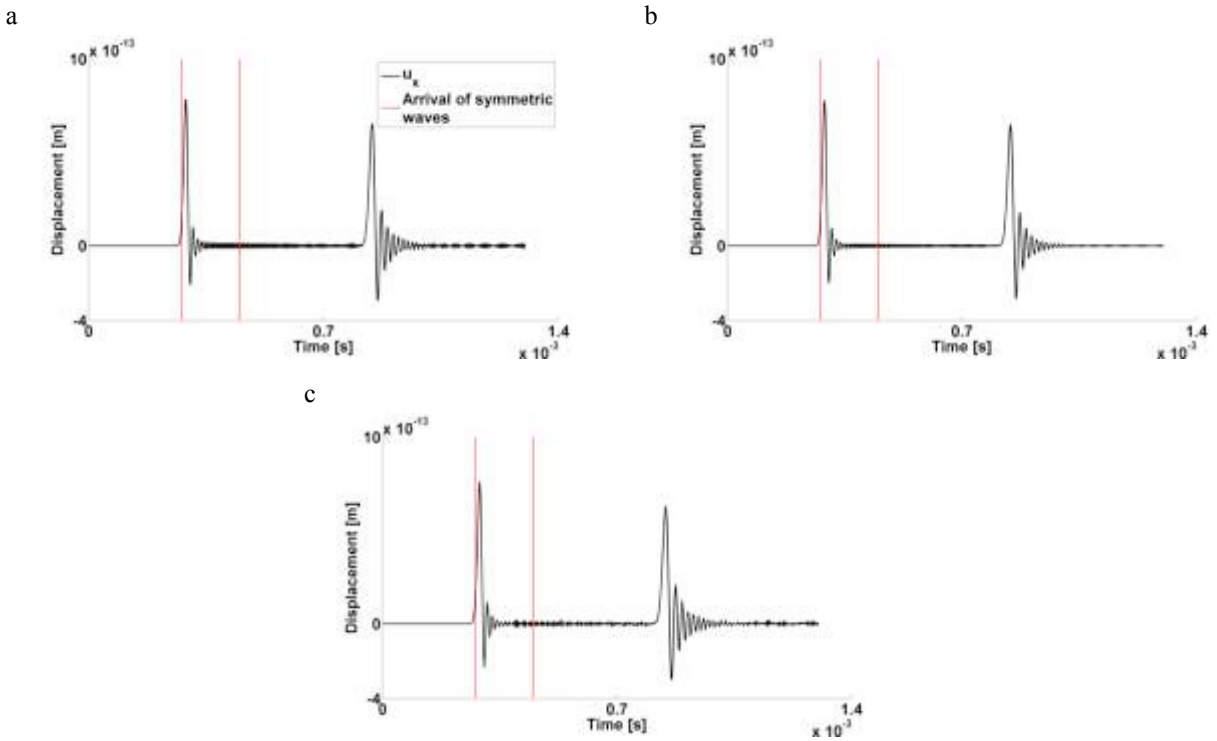

Fig. 8. Results of the second set of simulations for the 2D guided propagation case: (a) COMSOL; (b) APDL; (c) FEMAP.

Table 4. Second set of simulations for the 2D guided propagation case: analysis parameters and running times.

Employed code	Element edge [m] b_e	Time step [s] Δt	Number of elements	Running time [s]
COMSOL	$2.5 \cdot 10^{-3}$	$4.6 \cdot 10^{-7}$	9600	76
APDL	$2.5 \cdot 10^{-3}$	$4.6 \cdot 10^{-7}$	9600	188
FEMAP	$2.5 \cdot 10^{-3}$	$4.6 \cdot 10^{-7}$	9600	115

2.3. Guided waves propagation in a 3D domain

The last investigated instance regards the simulation of guided waves propagation in a three-dimensional numerical domain. The considered medium is a thin square plate with traction-free boundaries. An edge of 1.26 m and a thickness of 1 cm were chosen for the body. The same forcing function used for the bulk simulations was employed in this case. It acts as an out-of-plane force, applied at the upper left vertex of the top surface of the square. The bottom and right edges of the square were kept fixed while a symmetry condition was prescribed to the left and top ones. The force was set in order to selectively excite the anti-symmetric A_0 mode. The variable monitored was the out-of-plane displacement of a top surface point of the left edge of the plate, at a distance d = 0.79 m from the trigger site. The material properties of the body were the same considered in the previous sections. The solution of the Lamb problem for the present case of anti-symmetric propagation gave phase velocity $c_{ph,1}$ = 1897 m/s , group velocity $c_{g,1}$ = 2965 m/s and wavelength λ_1 = 0.038 m at 50 kHz. The chosen discretization criteria yield to $b_e = \lambda_1/10$ = 0.0038 m from (1), $\Delta t = 1/(20 \cdot 50 \cdot 10^3) = 1 \cdot 10^{-6}$ s from (3). The found spatial discretization is valid for the propagation directions. Since only the zero-order anti-symmetric mode was involved, the displacement field in the thickness of the plate is expected to have an almost monotonic behavior (with a positive and a negative peak at the outer points), justifying the adoption of no more than two divisions along that dimension in order to maintain an acceptable aspect ratio of the elements. These considerations led to the adoption of a prismatic mesh: two layers of triangular based prisms fill the volume of the numerical domain. The simulations were run from $t = 0$ to $t_{end} = 4 \cdot 10^{-4}$ s. Fig. 9 reports the monitored displacement obtained with COMSOL, APDL and FEMAP. The red line marks the arrival time of the anti-symmetric perturbation, expected at $t = d/c_{g,1} = 2.66 \cdot 10^{-4}$ s. The second bound was not reported since subsequent to the end of the simulation. It is clear from the figures that only FEMAP respected the velocity check. A practical way to deal with the time mismatch shown by COMSOL and APDL is to exploit the already described offset between spatial and temporal paces on waves velocities. After several trials, it was possible to find an acceptable solution only relaxing the condition given in (3), settling for 10 divisions per cycle. Another set of FE simulations was run, with a time step of $\Delta t = 2 \cdot 10^{-6}$ s. Fig. 10 report the monitored displacement over time for the second set of analyses. Signals obtained with COMSOL and APDL respect the check of velocities while an excessive delay can be noticed for FEMAP. Tables Table 5 and Table 6 summarize the analyses parameters and the running times for the 3D case. The time values reported for FEMAP refer to the case of a reduced output (limited to the sole displacement field) with respect to the other codes, since an issue of excessive memory occupation arose.

Table 5. First set of simulations for the 3D guided propagation case: analysis parameters and running times.

Employed code	Element edge [m] b_e	Time step [s] Δt	Number of elements	Running time [s]
COMSOL	$3.8 \cdot 10^{-3}$	$1 \cdot 10^{-6}$	530104	1331
APDL	$3.8 \cdot 10^{-3}$	$1 \cdot 10^{-6}$	763416	2297
FEMAP	$3.8 \cdot 10^{-3}$	$1 \cdot 10^{-6}$	440896	1137 (reduced output)

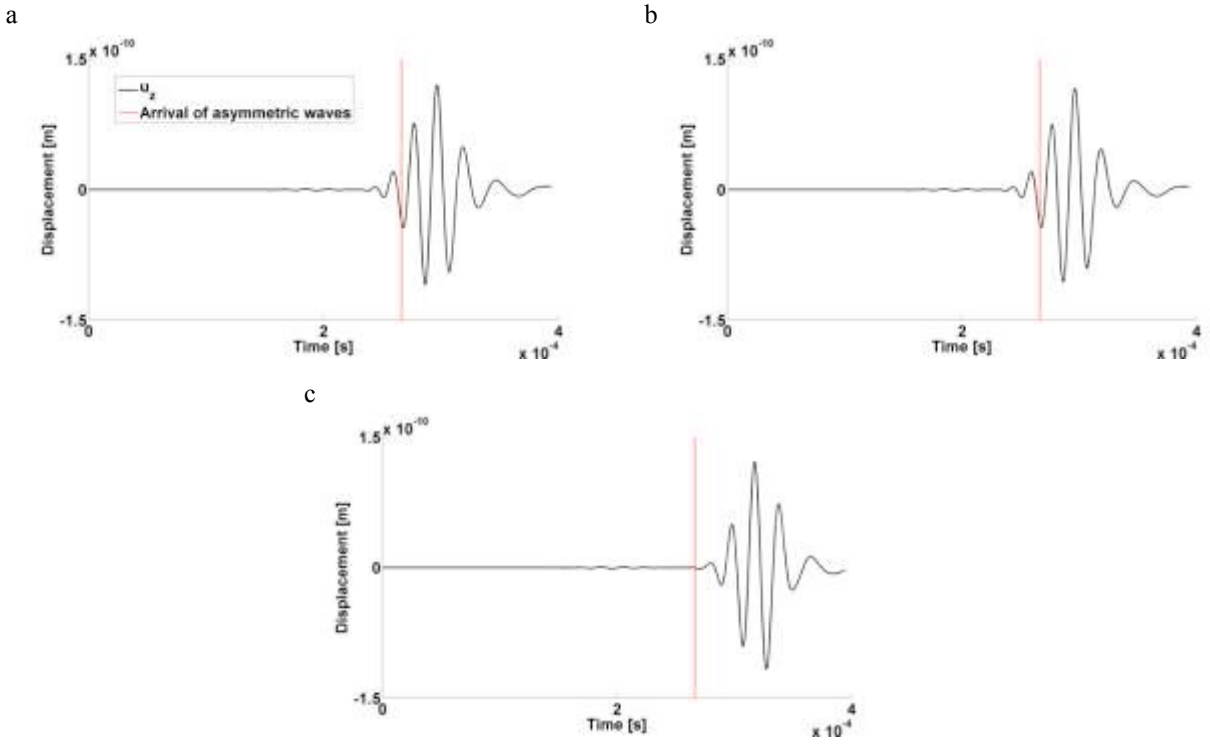

Fig. 9. Results of the first set of simulations for the 3D guided propagation case: (a) COMSOL; (b) APDL; (c) FEMAP.

Table 6. Second set of simulations for the 3D guided propagation case: analysis parameters and running times.

Employed code	Element edge [m] b_e	Time step [s] Δt	Number of elements	Running time [s]
COMSOL	$3.8 \cdot 10^{-3}$	$2 \cdot 10^{-6}$	530104	751
APDL	$3.8 \cdot 10^{-3}$	$2 \cdot 10^{-6}$	763416	1139
FEMAP	$3.8 \cdot 10^{-3}$	$2 \cdot 10^{-6}$	440896	711 (reduced output)

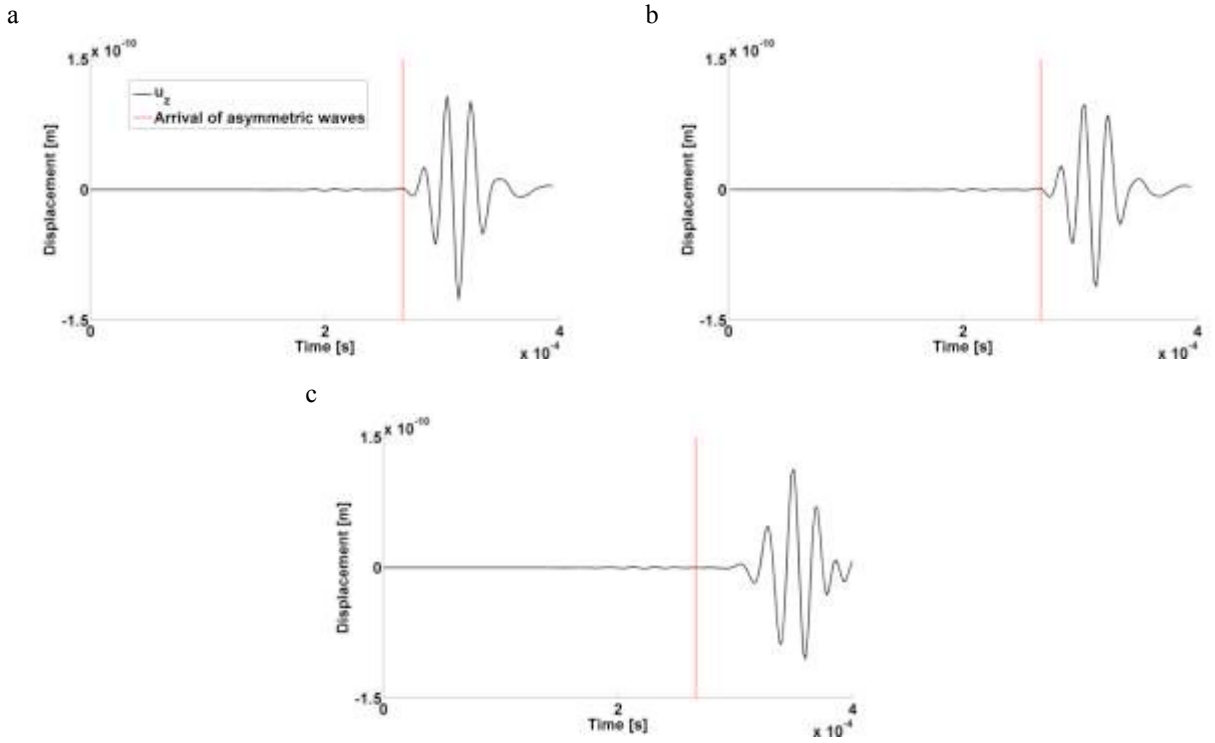

Fig. 10. Results of the second set of simulations for the 3D guided propagation case: (a) COMSOL; (b) APDL; (c) FEMAP.

2.4. High Performance Computing

Running times can be reduced with the employment of High Performance Computing (HPC). The machine utilized for the purpose was a Server Dell PowerEdge R940, 4 CPU Intel(R) Xeon(R) Gold 6152 CPU @ 2.10GHz, 256 GB of RAM, 2 TB of disk space and 88 working cores. The obtained speed-up is shown for the case of ANSYS APDL. The graph in Fig. 11 shows the dependency of running time on the number of active cores for the three-dimensional case of waves propagation. As expected, time spent to run the analyses decreases with the number of cores, exhibiting a tendency to saturation for more than 30 cores. Although the burden on each core reduces when their number is augmented, data exchange starts playing a growing role, which explains the flattening of the curve in the graph. When shifting from 5 to 88 cores, running time plummets from 43 to 6 minutes, with a time saving of 86%.

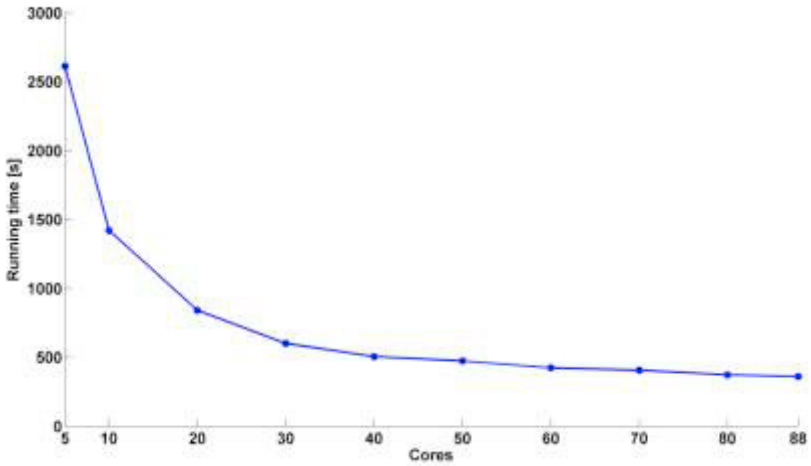

Fig. 11. Running time vs number of active cores for the HPC tests.

3. Conclusions

In the latest decades, ultrasonic guided waves proved to be a valuable tool for the non-destructive assessment of structures. The physics behind their propagation is complex and analytical models are possible only for simplified cases. The only feasible way for an accurate study of their transmission through variously-shaped domains relies on FEM analyses. Although FEM is well suited for the simulation of complex domains, transient analyses come along with the matter of spatial and temporal discretization. In this paper different FEM codes were tested against different scenarios of waves propagation. Three widely-used commercial tools: COMSOL, ANSYS APDL and FEMAP with NX NASTRAN were employed to model bulk and guided ultrasonic waves propagation in two-dimensional models. A further instance of guided propagation in a three-dimensional medium was also considered. Numerical domains used for guided waves transmission were shaped as thin plates, fulfilling the requirements of the Lamb problem. Dispersion curves supplied the group velocities for the waves, allowing for a simple but effective check of numerical results. APDL and FEMAP proved to be more robust since they were able to give the correct results for different time and space resolutions. As regards running times, COMSOL outperformed the other codes for all the considered instances, on the other hand it showed a major sensitivity to the adopted discretization, being waves velocities more affected by the spatial and temporal paces. A proper ratio between them needs to be found in order to avoid an inaccurate propagation of waves through the numerical domain.

High Performance Computing (HPC) was tested for the three-dimensional case using APDL. A time saving of 86% was observed when increasing the working cores from 5 to 88.

References

Lowe, MSJ., Alleyne, DN., Cawley, P., 1998. Defect detection in pipes using guided waves. Ultrasonics 36, 147-154

Leckey, CAC., Wheeler, KR., Hafiychuk, VN., Hafiychuk, H., Timuçin, DA., 2018. Simulation of guided-wave ultrasound propagation in composite laminates: benchmark comparisons of numerical coded and experiment. Ultrasonics 84, 187-200

Rose, JL., 2014. Ultrasonic guided waves in solid media. Cambridge University Press, New York USA

Gavrić, L., 1994. Finite element computation of dispersion properties of thin-walled waveguides. Journal of Sound and Vibration 173(1), 113-124

Gavrić, L., 1995. Computation of propagative waves in free rail using a finite element technique. Journal of Sound and Vibration 185(3), 531-543

Wilcox, P., Evans, M., Diligent, O., Lowe, M., Cawley, P., 2002. Dispersion and excitability of guided acoustic waves in isotropic beams with arbitrary cross section. Review of Quantitative Nondestructive Evaluation 21, 203-210

Bartoli, I., Marzani, A., Lanza di Scalea, F., Viola, E., 2006. Modeling wave propagation in damped waveguides of arbitrary cross-section. Journal of Sound and Vibration 295(3), 685-707

Marzani, A., Viola, E., Bartoli, I., Lanza di Scalea, F., Rizzo, P., 2008. A semi-analytical finite element formulation for modeling stress wave propagation in axisymmetric damped waveguides. Journal of Sound and Vibration 318, 488-505

Bartoli, I., Lanza di Scalea, F., Fateh, M., Viola, E., 2005. Modeling guided wave propagation with applications to the long-range defect detection in railroads tracks. NDT&E International 38, 325-334

Moser, F., Jacobs, LJ., Qu, J., 1999. Modeling elastic wave propagation in waveguides with the finite element method. NDT&E International 32, 225-234